Detecting Spin-Polarized Currents in Ballistic Nanostructures

R. M. Potok,[1] J. A. Folk,[1,2] C. M. Marcus,[1] and V. Umansky[3]
[1]*Department of Physics, Harvard University, Cambridge, Massachusetts 02138*
[2]*Department of Physics, Stanford University, Stanford, California 94305*
[3]*Braun Center for Submicron Research, Weizmann Institute of Science, Rehovot 76100, Israel*
(Received 19 June 2002; published 9 December 2002)

We demonstrate a mesoscopic spin polarizer/analyzer system that allows the spin polarization of current from a quantum point contact in a large in-plane magnetic field to be measured. A transverse electron focusing geometry is used to couple current from an emitter point contact into a collector point contact. At large in-plane fields, with the point contacts biased to transmit only a single spin ($g < e^2/h$), the voltage across the collector depends on the spin polarization of the current incident on it. Spin polarizations of $> 70\%$ are found for both emitter and collector at 300 mK and 7 T in-plane field.

DOI: 10.1103/PhysRevLett.89.266602 PACS numbers: 72.25.Dc, 72.25.Hg, 73.23.Ad

The detection of electron spin in mesoscopic systems has been the aim of extensive experimental efforts for many years. The ability to prepare, manipulate, and measure electron spin in solid state systems [1] not only provides a new tool to investigate the physics of mesoscopic structures [2], but also provides hope that these capabilities may open the way for applications in spintronics and quantum information processing [3]. However, the long coherence times [4] that make electron spin interesting arise fundamentally from the weak coupling of spin to the environment, and this makes the task of measuring spin difficult.

In this Letter we demonstrate a technique to measure spin currents by converting the problem into the easier one of measuring currents of electrical charge. At low field and low temperature, a narrow constriction in a 2D electron gas (2DEG), a quantum point contact (QPC) [see Fig. 1(a)], transmits through two spin degenerate channels, producing conductance plateaus at integer multiples of $2e^2/h$. When a large in-plane magnetic field is applied, the degeneracy is lifted and conductance becomes quantized in multiples of $1e^2/h$ [Fig. 1(b)] [5,6]. While the electrons emitted from an e^2/h plateau are widely believed to be spin polarized, this has not been verified experimentally to our knowledge. One key result of this Letter is the demonstration that point contacts do operate as emitters and detectors of spin current, and therefore allow the detection of spin polarization to be accomplished by simply measuring electrical resistance.

Our experiment is based on a technique known as transverse electron focusing [7], which has been used previously to study phenomena ranging from anisotropy in the band structure of metals [8,9] and semiconductors [10,11] to composite fermions in the fractional quantum Hall regime [12]. This device geometry [Fig. 1(a)] allows electrons from a spin-polarizing emitter—in this case a QPC—to be coupled into a second QPC serving as a spin-sensitive collector. A magnetic field, $B_\perp$, applied perpendicular to the 2DEG plane, bends and focuses ballistic electron trajectories from the emitter to the collector, resulting in peaks in the base-collector voltage [Figs. 1(c) and 1(d)] whenever the spacing between point contacts is an integer multiple of the cyclotron diameter, $m^* v_F/eB_\perp$, where m^* is the effective electron mass and v_F the Fermi velocity.

The coupling efficiency between emitter and collector can be quite high in clean 2DEG materials, allowing the two QPCs to be separated by several microns. This separation is useful for measuring spin physics in mesoscopic structures because it allows spin measurements of the emitted current to be decoupled from the details of the emitting device under test, simplifying the interpretation of results. A further advantage of a focusing geometry is that spin detection occurs very quickly (< 10 ps) after the polarized electrons are emitted, leaving little time for spin relaxation.

In the present experiment, the focusing signal is measured as a voltage between collector and base regions, with fixed current applied between emitter and base [Fig. 1(a)]. With the collector configured as a voltage probe, current injected ballistically into the collector region at the focusing condition must flow back into the base region, giving rise to a voltage $V_c = I_c/g_c$ between collector and base, where I_c is the current injected into the collector and g_c is the conductance of the collector point contact. For this experiment both point contacts are kept at or below one channel of conductance; therefore the collector voltage may be written in terms of the transmission of the collector point contact, T_c (≤ 1), as $V_c = (2e^2/h)^{-1} I_c/T_c$ in the spinless case.

To analyze how spin polarization affects the base-collector voltage, we assume $I_{\downarrow c} + I_{\uparrow c} = \alpha(I_{\downarrow e} T_{\downarrow c} + I_{\uparrow e} T_{\uparrow c})$, where I_e is the emitter current, and α is a spin-independent efficiency parameter reflecting imperfections in the focusing process such as scattering from impurities ($0 < \alpha < 1$). In the absence of spin effects ($T_{\uparrow c} = T_{\downarrow c}$), one then expects V_c to be independent of g_c, although different settings of the point contact may in

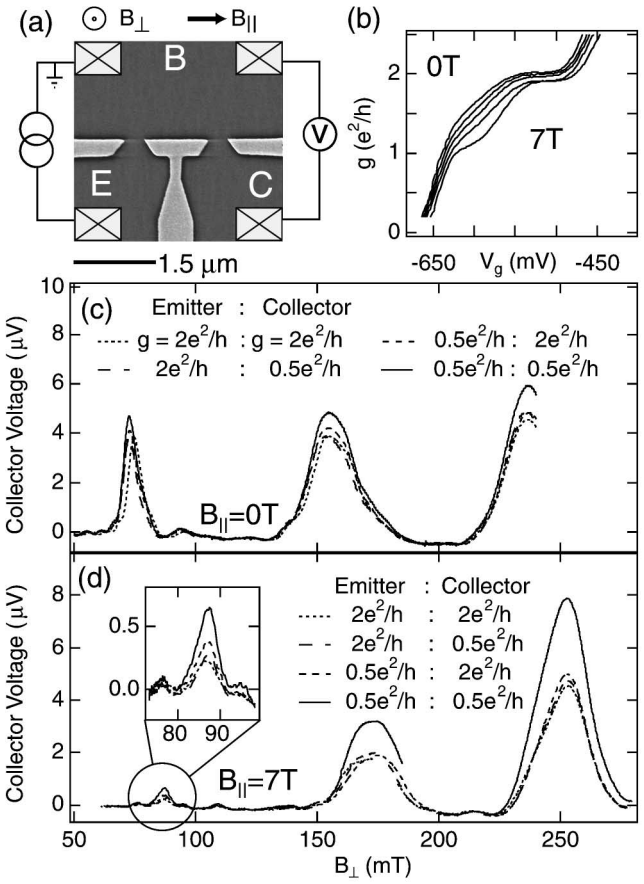

FIG. 1. (a) Scanning electron micrograph of a device similar to the one measured in this experiment, two quantum point contacts in a transverse focusing geometry with perpendicular ($B_\perp$) and in-plane ($B_\parallel$) magnetic fields oriented as shown. With a fixed current applied between emitter (E) and base (B), the voltage between base and collector (C) showed focusing peaks as a function of $B_\perp$. (b) At $T = 300$ mK, both point contacts showed conductance quantized in units of $2e^2/h$ at $B_\parallel = 0$, and in units of e^2/h at large $B_\parallel$. (c) At $B_\parallel = 0$, the collector voltage was nearly independent of the conductances of the two point contacts. The last focusing peak is cut off due to current limitations of the perpendicular field solenoid. (d) At $B_\parallel = 7$ T the focusing peaks were enhanced only when both emitter and collector are set to $g = 0.5e^2/h$. The enhancement demonstrates that both emitter and detector are spin selective, by [Eq. (1)].

practice affect α. Because I_e is fixed, V_c is also independent of the emitter conductance, g_e.

Taking into account different transmissions for the two spin channels, however, one expects the voltage on the collector to double if both emitter and collector pass the same spin, or drop to zero if the two pass opposite spins. This conclusion assumes that a spin-polarized current injected into the collector region will lose all polarization before flowing out again. Under these conditions, the collector voltage generally depends on the polarization of the emitter current $P_e = (I_\uparrow - I_\downarrow)/(I_\uparrow + I_\downarrow)$ and the spin selectivity of the collector $P_c = (T_\uparrow - T_\downarrow)/(T_\uparrow + T_\downarrow)$ in the following simple way [13]:

$$V_c = \alpha \frac{h}{2e^2} I_e (1 + P_e P_c). \quad (1)$$

Note from Eq. (1) that collinear and complete spin polarization ($P_e = 1$) and spin selectivity ($P_c = 1$) gives a collector voltage twice as large as when *either* emitter or collector are not spin polarized.

The focusing device was fabricated on a high-mobility 2DEG formed at the interface of a $GaAs/Al_{0.36}Ga_{0.64}As$ heterostructure, defined using Cr/Au surface depletion gates patterned by electron-beam lithography, and contacted with nonmagnetic (PtAuGe) ohmic contacts. The 2DEG was 26 nm from the Si delta-doped layer ($n_{Si} = 2.5 \times 10^{12}$ cm^{-2}) and 102 nm below the wafer surface. Mobility of the unpatterned 2DEG was 5.5×10^6 cm^2/V s in the dark, limited mostly by remote impurity scattering in the relatively shallow structure, with an estimated background impurity level $< 5 \times 10^{13}$ cm^{-3}. With an electron density of $\sim 1.3 \times 10^{11}$ cm^{-2}, the transport mean free path was ~ 45 μm, much greater than the distance (1.5 μm) between emitter and collector point contacts. The Fermi velocity associated with this density is $v_F = 2 \times 10^7$ cm/s, consistent with the observed ~ 80 mT spacing between focusing peaks.

Measurements were performed in a ^{3}He cryostat with a base temperature of 300 mK. A conventional superconducting solenoid was used to generate in-plane fields, $B_\parallel$, and a smaller superconducting coil wound on the refrigerator vacuum can allowed fine control up to ~ 250 mT of the perpendicular field, $B_\perp$ [14]. $B_\parallel$ was oriented along the axis between the two point contacts, as shown in Fig. 1(a).

Independent ac current biases of 1 nA were applied between base and emitter (17 Hz), and base and collector (43 Hz), allowing simultaneous lock-in measurement of the emitter conductance (base-emitter voltage at 17 Hz), collector conductance (base-collector voltage at 43 Hz), and the focusing signal (base-collector voltage at 17 Hz). The base-collector current bias was found to have no effect on the focusing signal. Additionally, the focusing signal was found to be linear in base-emitter current for the small currents used in this measurement.

The qualitative behavior of the focusing peaks did not change upon thermal cycling. Although all of the data presented come from a single device, results were confirmed in a similar device on the same heterostructure. Statistics leading to estimates of typical polarization values discussed at the end of the paper were gathered over five settings of point contact voltages (for fixed conductance) for each of the three focusing peaks. Data from the three focusing peaks showed consistent behavior.

Spin polarized emission and detection were measured by comparing the height of the focusing peak for various

conductances of the emitter and collector point contacts. At $B_{\|} = 0$, where no static spin polarization is expected, the focusing signal was found to be nearly independent of the conductances of both emitter and collector point contacts, as shown in Fig. 1(c). In contrast, at $B_{\|} = 7$ T, the focusing signal observed when both the emitter and collector point contacts were set well below $2e^2/h$ was larger by a factor of $\sim$1.7 compared to the signal when either emitter or collector was set to $2e^2/h$, as seen in Fig. 1(d).

To normalize for overall variations in transmission through the bulk from the emitter to the collector, the focusing signal can be expressed as a ratio normalized by the value when both the emitter and collector are set to $2e^2/h$. We denote the point contact settings as $(x{:}y)$ where x (y) is the emitter (collector) conductance, in units of e^2/h. Ratios are then denoted $(x{:}y)/(2{:}2)$.

Figures 2 and 3 show the focusing signal ratios for the third focusing peak ($B_{\perp} \sim 230$–250 mT), chosen because its height and structure in the (2:2) condition were less sensitive to $B_{\|}$ and small variations in point contact tuning compared to the first and second peaks. Although all curves shown in this paper were for the third focusing peak, spin polarization extracted from the first and second focusing peaks gave similar results.

Figure 2(a) shows that only the ratio (0.5:0.5)/(2:2) grows with $B_{\|}$, reaching a value $\sim$2 at 7 T, while the other ratios, (2:0.5)/(2:2) and (0.5:2)/(2:2), are essentially independent of in-plane field, as expected from Eq. (1) if no spin selectivity exists when the conductance is $2e^2/h$. At $B_{\|} = 0$, we find (0.5:0.5)/(2:2) $\sim$ 1.4, rather than the expected 1.0, for this particular setting of the point contacts.

Temperature dependences of the (0.5:0.5)/(2:2) ratio are shown in Fig. 2(b) for a different cooldown. At $B_{\|} =$ 7 T, the ratio (0.5:0.5)/(2:2) decreases from $\sim$2.2 at $T =$ 300 mK to a zero-field value of 1.4 above 2 K. Note that 2 K is roughly the temperature at which $g\mu B_{\|}/kT \sim 1$, using the GaAs g factor $g = -0.44$. At $B_{\|} = 0$, the ratio (0.5:0.5)/(2:2) remains near 1.4, with only a weak temperature dependence up to 6 K.

The inset of Fig. 2(b) shows that the focusing data at several $B_{\|}$ scale to a single curve when plotted as a function of $kT/g\mu B_{\|}$, suggesting that both spin-polarized emission and spin-selective detection arise from an energy splitting that is linear in $B_{\|}$. A simple model that accounts roughly for the observed scaling of the focusing signal assumes that the point contact transmission, $T(E)$, is 0 for $E < E_0$, and 1 for $E > E_0$, where E is the electron kinetic energy and E_0 is a gate-voltage-dependent threshold. Spin selectivity then results from the Zeeman splitting of the two spin subbands, and is reduced by thermal broadening. Except for a vertical offset of $\sim$0.4, this simple model agrees reasonably well with the data [Fig. 2(b), inset].

Figure 3(a) shows the evolution of spin selectivity in the collector point contact as a function of its conductance. At $B_{\|} = 6$ T, with the emitter point contact set to $0.5e^2/h$, the collector point contact is swept from $2e^2/h$ to 0. The focusing signal increases as the collector point contact conductance is reduced below $2e^2/h$, saturating only well into the tunneling regime, below $\sim 0.5e^2/h$. For this reason we use emitter and collector conductances of $0.5e^2/h$ in all figures for the spin-selective cases (although the qualitative behavior of the data was essentially the same here as on the $1e^2/h$ plateau). Similar to the effect seen in Fig. 2(b), spin selectivity decreases with increasing temperature, approaching the zero-field curve at 1.3 K.

Figure 3(b) shows the same measurement taken at $B_{\|} = 0$. The focusing peak rises slightly when both point contacts are set below one spin degenerate channel.

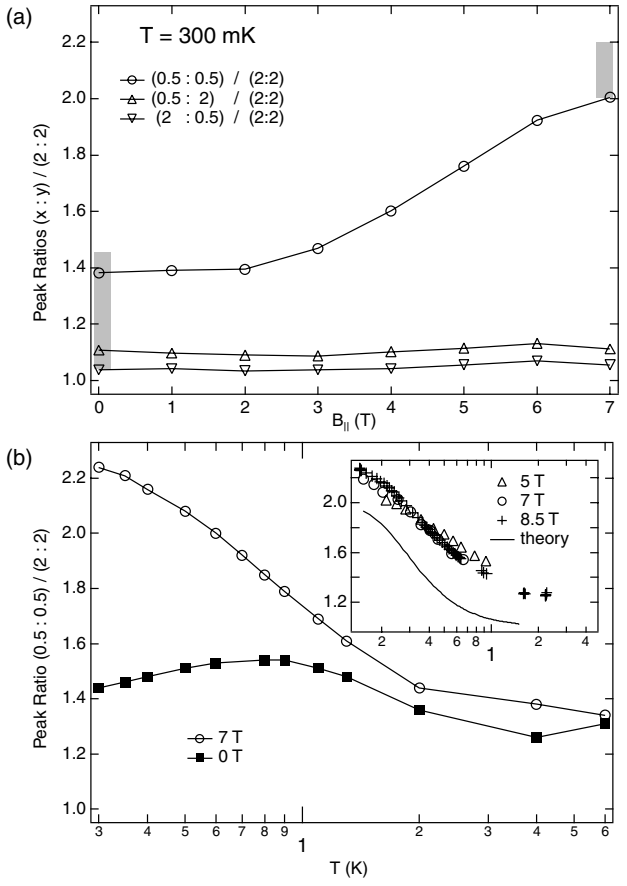

FIG. 2. (a) The height of the third focusing peak as a function of $B_{\|}$ for different conductances of the point contacts $(x{:}y)$, where x is the emitter conductance and y is the collector conductance (in units of e^2/h), all normalized by the (2:2) focusing peak height. According to Eq. (1), a factor of 2 in the ratio indicates fully spin polarized emission and detection. Grey shaded boxes indicate typical ranges (see text) of (0.5:0.5)/(2:2) ratio. (b) Temperature dependence of the ratio of focusing signals (0.5:0.5)/(2:2) for $B_{\|} = 7$ and 0 T. (a) and (b) are from different cooldowns. Inset: Ratio (0.5:0.5)/(2:2) for $B_{\|} = 5, 7$, and 8.5 T plotted as a function of the scaled temperature $kT/g\mu B_{\|}$. The solid curve is the prediction of a simple model (see text) that accounts for only thermal broadening in the leads.

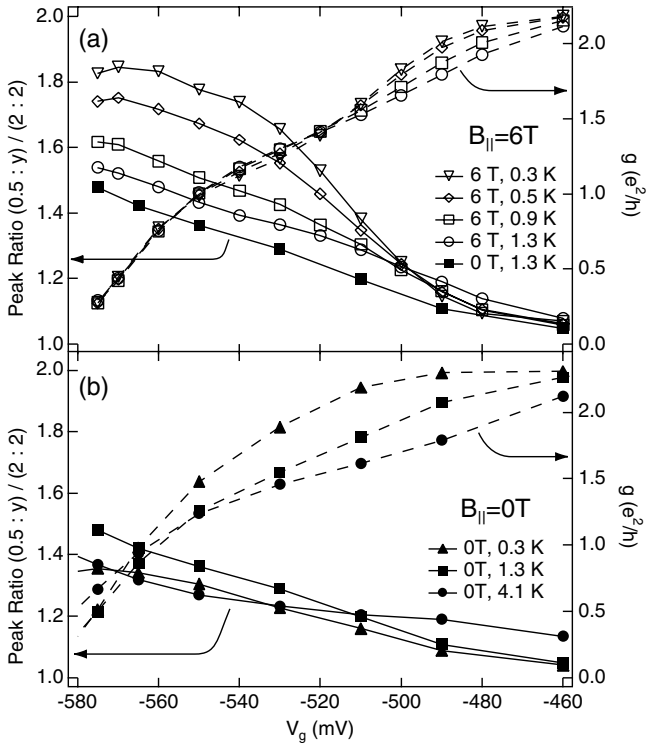

FIG. 3. (a) Focusing signal ratio $(0.5{:}y)/(2{:}2)$ and collector conductance g at $B_{\|} = 6$ T as a function of the voltage applied to one of the collector gates, with the emitter fixed at $g = 0.5e^2/h$. This shows the onset of spin selectivity as the collector point contact is brought into the tunneling regime, $g < 2e^2/h$. (b) The same data taken at $B_{\|} = 0$, showing little temperature dependence up to 4 K. A mild 0.7 structure in the conductance becomes more prominent at 1.3 K.

Unlike at high field, however, the increase of the focusing signal is very gradual as the point contact is pinched off. In addition, temperature has only a weak effect.

As mentioned above, both the low and high field ratios $(0.5{:}0.5)/(2{:}2)$ were typically measured to be larger than their ideal theoretical values of 1 and 2, respectively. Sampled over multiple thermal cycles, several gate voltage settings (shifting the point contact centers by $\sim$100 nm), and different focusing peaks, the ratio at $B_{\|} = 0$ varied between 1.0 and 1.6, with an average value of 1.2 and a standard deviation $\sigma = 0.2$. The average value of the ratio at $B_{\|} = 7$ T was 2.1, with $\sigma = 0.1$. This represents an increase from low to high field by a factor of 1.7 ± 0.3, so from Eq. (1) one finds $P_e P_c = 0.7 \pm 0.3$. Because neither P_e nor P_c can be greater than 1, this then implies that both P_e and P_c are greater than 0.7 ± 0.3, and under the assumption that $P_e \sim P_c$ it implies that $P_e, P_c \gtrsim 0.8$.

Both point contacts display a modest amount of zero-field 0.7 structure [15,16], as seen in Figs. 1(b) and 3(b). Although a static spin polarization associated with 0.7 structure would be consistent with our larger-than-one ratio $(0.5{:}0.5)/(2{:}2)$ at zero field, this explanation is not consistent with an enhanced ratio found *both* at zero field and high field. Rather, we believe the enhancement is due to a slight dependence of α on QPC settings in the regime $(T_c, T_e) < 1$. This explanation is consistent with the weak temperature dependence of the zero-field ratio up to 4 K.

An unexplained feature of our data is the relative suppression of the lower-index focusing peaks, particularly the first peak, in a large in-plane field, as seen in Figs. 1(c) and 1(d). This effect was observed over multiple cooldowns and for all point contact positions. The effect is not readily explained as a field-dependent change in the scattering rate, as neither the bulk mobility, nor the width of the focusing peak is affected. Also, the effect is not obviously related to spin, as it occurred for both polarized and unpolarized point contacts. All peaks are included in the statistics presented.

In conclusion, we have developed a new method for creating and remotely detecting spin currents using quantum point contacts. In future work, this technique may be applied to more subtle mesoscopic spin systems such as measuring spin currents from open or Coulomb-blockaded quantum dots, or directly measuring spin precession due to a spin-orbit interaction.

We acknowledge valuable discussions with H. Bruus, S. Cronenwett, A. Johnson, and H. Lynch. This work was supported in part by The Darpa SpinS and QuIST programs and the ARO-MURI DAAD-19-99-1-0215. R. M. P. acknowledges support from the ARO Graduate Research program, and J. A. F. acknowledges support from Stanford University.

[1] R. Fiederling *et al.*, Nature (London) **402**, 787 (1999).
[2] A. S. Sachrajda *et al.*, Physica (Amsterdam) **10E**, 493 (2001).
[3] *Semiconductor Spintronics and Quantum Computation*, edited by D. D. Awschalom, D. Loss, and N. Samarth (Springer-Verlag, Berlin, 2002).
[4] J. M. Kikkawa and D. D. Awschalom, Phys. Rev. Lett. **80**, 4313 (1998).
[5] D. A. Wharam *et al.*, J. Phys. C **21**, L209 (1988).
[6] B. J. van Wees *et al.*, Phys. Rev. B **38**, 3625 (1988).
[7] H. van Houten *et al.*, Phys. Rev. B **39**, 8556 (1989).
[8] Yu. V. Sharvin and N. I. Bogatina, Zh. Eksp. Teor. Fiz. **56**, 772 (1969).
[9] V. S. Tsoi and I. I. Razgonov, Zh. Eksp. Teor. Fiz. **74**, 1137 (1978).
[10] G. Goldoni and A. Fasolini, Phys. Rev. B **44**, 8369 (1991).
[11] K. Ohtsuka *et al.*, Physica (Amsterdam) **251B**, 780 (1998).
[12] V. J. Goldman, B. Su, and J. K. Jain, Phys. Rev. Lett. **72**, 2065 (1994).
[13] We have, including spin, $V_c = (I_{c\uparrow} + I_{c\downarrow})/g_c$, $I_{c\sigma} \propto I_{e\sigma} T_{c\sigma}$, and $g_c = (T_{c\uparrow} + T_{c\downarrow})(e^2/h)$, so $V_c \propto (I_{e\uparrow} T_{c\uparrow} + I_{e\downarrow} T_{c\downarrow})/(T_{c\uparrow} + T_{c\downarrow})$. H. Bruus, J. A. Folk, A. C. Johnson, and R. M. Potok (unpublished).
[14] J. A. Folk *et al.*, Phys. Rev. Lett. **86**, 2102 (2001).
[15] K. J. Thomas *et al.*, Phys. Rev. Lett. **77**, 135 (1996).
[16] S. M. Cronenwett *et al.*, Phys. Rev. Lett. **88**, 226805 (2002).